An Investigation on Interaction between 14mer DNA Oligonucleotide and CTAB by Fluorescence and Fluorescence Resonance Energy Transfer Studies

Deenan Santhiya and Souvik Maiti*

Institute for Genomics and Integrative Biology, CSIR, Mall Road, Delhi 110 007, India

Received: October 5, 2009; Revised Manuscript Received: May 5, 2010

Possible interaction mechanisms between oligonucleotide (DNA) of 14 base pairs with cetyl trimethyl ammonium bromide (CTAB) were postulated based on fluorescence and fluorescence resonance energy transfer (FRET) studies. Detailed FRET investigations were carried out by fluorometric titrations of the surfactant with various oligonucleotide duplexes with 5′-tagged fluorescein (donor) (D_D), 5′-tagged TAMRA (acceptor) (D_A) and both (D_{DA}). In general, fluorescence spectra of the duplexes (D_D, D_A and D_{DA}) revealed a reduction in the fluorescence intensities of 5′-fluorescein as well as 5′-TAMRA and thereafter an attainment of saturation with increase in the surfactant concentration. The observed changes in the oligonucleotide fluorescence intensities for the duplexes under investigation could be attributed to the microenvironmental changes during the oligonucleotide−CTAB interaction. Considering together, it appeared that the interaction is a three-stage process, wherein the initial addition of surfactant caused neutralization of the 14mer at $Z^1_{\pm} = 0.8$, which is manifested by a slight reduction in fluorescence intensity. Further, addition of the surfactant molecules sharply reduced the fluorescence intensity of the oligonucleotide depicting oligonucleotide induced self-assembly until the second break point ($Z^2_{\pm} = 1.7$). From the second break point, a striking resonance energy transfer was observed from donor to acceptor, which revealed shortening of distance between 5′ ends of the oligonucleotides that attained a saturation at $Z^3_{\pm} = 2.5$. Similar three-stage interaction of oligonucleotide with the surfactant has also been observed through fluorometric titrations in the presence of NaCl. However, in the presence of the salt, neutralization of oligonucleotide, surfactant aggregation and FRET occurred at higher charge ratios due to the screening effect of Na^+ ions followed by an increase in critical association concentration (CAC) of the surfactant. Overall, investigations probe possible structural changes in the 14mer oligonucleotide−CTAB complex upon increase in the surfactant concentration.

Introduction

In this genomic era, DNA that contains the genetic instructions for the development and functioning of living organisms has become a center of attraction for many researchers. Most importantly, in biomedical research, sequencing of the human genome has opened up enormous possibilities for curing a variety of diseases, including genetic diseases, cancers, cardiovascular diseases and so on, by gene therapy.[1] Gene therapy involves therapeutic gene transfer into specific cells and its subsequent release into the nucleus using either viral or nonviral vectors.[2−9] The majority of clinical trials use genetically modified viral vectors for gene delivery, but viral methods have raised questions about medical risks, such as insertional mutagenesis, the possibility of serious immune reactions and the risk of transferring replication-competent viral particles. Additionally, gene transfer capacity of the viral vectors is limited to 40 kbp. Hence, a safer alternative for transfection of DNA using nonviral vectors has generated increasing interest.[10,11] The nonviral vectors are formed by the self-assembly of DNA and complexing agents like polyamines, multivalent metal cations, hydrophilic polymers, cationic polymers, cationic liposomes and cationic as well as nonionic surfactants.[1] In addition to neutralizing effects, the nonviral complexing agents are also demonstrated to condense DNA from an extended coil into a variety of compact structures like toroids, spheroids and rods.[12−14] So far, such compacted DNA with charge reduction is believed to facilitate gene transfer through the cellular membrane. However, investigations of DNA−membrane interactions are hindered by difficulties involved in the isolation of DNA in compact form. Hence, to understand the potential contribution of various factors influencing DNA compaction, in vitro DNA condensation experiments using membrane like systems made of cationic surfactants are designed. A number of researchers have shown that in the DNA−surfactant complexes the cationic surfactant molecules bind to the DNA chains through electrostatic interactions. In addition to this the hydrophobic moieties of the surfactant molecules stabilize the complex through the hydrophobic interactions with the DNA.[15−17]

Based on the studies carried out on the compaction of double-stranded DNA (ds-DNA) by cationic surfactants, using fluorescence microscopy, three distinguishable regimes of the DNA compaction process are highlighted, depending on the concentration of the cationic surfactant.[1,18−24] In the absence of surfactant, DNA molecules in solution exist in extended (coil) conformation with relatively slow wormlike motion. At sufficiently high concentrations of the surfactant, DNA molecules are present in mere compact state as globules exhibiting a larger mobility in solution. As one can speculate, DNA exists in both coil and globular conformations for intermediate surfactant concentrations.[1,18−24]

In this study, we demonstrate the binding mechanism of cationic surfactant cetyl trimethylammonium bromide (CTAB) with oligonucleotide using fluorescence and fluorescence reso-

* To whom correspondence should be addressed. E-mail: souvik@igib.res.in. Fax: +91 11 27667471.

10.1021/jp909522r
Published on Web 05/17/2010

nance energy transfer (FRET) methods. FRET is a widely used technique for the quantification of molecular dynamics in phenomena like protein−protein interaction, protein−DNA interactions and protein conformational changes. In order to monitor complex formation between two molecules, one of the molecules is labeled with a donor fluorophore and the other with an acceptor fluorophore. When the donor and acceptor are in close proximity (1−10 nm) due to complex formation, the predominantly observed emission is that of the acceptor because of intermolecular FRET from donor to acceptor, whereas, in the absence of complex formation, FRET from donor to acceptor cannot occur, and donor emission predominates. Considering the therapeutic potential of small synthetic oligonucleotides in manipulation of gene expression for the treatment of certain diseases, we studied synthetic 14mer DNA oligonucleotide−CTAB interactions. For FRET investigations, the oligonucleotide was tagged at 5′ with fluorescein (strand I) and tetramethylrhodamine (TAMRA) (strand II) and fluorometric titrations were performed with CTAB both in the presence and in the absence of NaCl. Similarly, fluorometric titrations were also carried out for oligonucleotides 5′-tagged with either fluorescein or TAMRA. The interaction was investigated by ethidium bromide exclusion and gel electrophoresis studies in the absence and in the presence of NaCl.

Materials and Methods

Materials. The unlabeled 14mer oligonucleotide strand I (5′-GATGTTCACTCCAG-3′) and strand II (5′-CTGGAGTGAACATC-3′) were supplied by SBS-Genetech. The GC content of the oligonucleotide was reported as 50% by the manufacturer. The 14mer strand I oligonucleotide (5′-GATGTTCACTCCAG-3′) 5′-tagged with fluorescein and its corresponding complementary strand II (5′-CTGGAGTGAACATC-3′) 5′-tagged with tetramethylrhodamine (TAMRA) were obtained from Sigma. The concentrations of strand I and strand II were determined by extrapolation of tabulated values of the monomer bases at 25 °C,[25,26] and the concentrations of labeled strands were determined based on optical density (OD) values provided by the manufacturer.

The duplex oligonucleotide preparation was carried out as follows:

Equimolar concentrations of both untagged strands of oligonucleotide were mixed at room temperature, and the mixture was heated to 95 °C for 10 min and slowly cooled to room temperature in 30 min to obtain untagged duplex (D_0). Similarly, labeled duplexes were prepared as given below: For the preparation of 5′-fluorescein labeled duplex (D_D), 5′-fluorescein tagged strand I was mixed with untagged strand II. 5′-TAMRA tagged duplex (D_A) was made by mixing unlabeled strand I and 5′-TAMRA tagged strand II. Dual tagged oligonucleotide (D_{DA}) was prepared by using 5′-fluorescein tagged strand I and 5′-TAMRA labeled strand II.

All the experiments were carried out using 10 mM sodium phosphate buffer at pH 7.0. Based on the phosphate charges of oligonucleotide, 1 μM oligonucleotide was considered to be equivalent to 26 μM (one 14mer single strand oligonucleotides contains 13 phosphate groups) phosphate charge. Analytical grade CTAB was obtained from Spectrochem (India), CTAB stock solutions were prepared by dissolving the required amount of CTAB in a known volume of warm phosphate buffer solution (18.2 mg/10 mL), and the corresponding concentrations were determined gravimetrically. The structure of CTAB is shown in Figure 1. All the other reagents used were of AR grade purity. Milli-Q water was used for all the experiments.

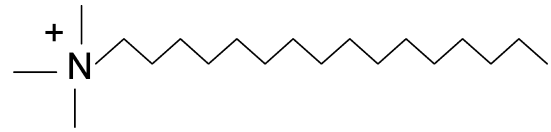

Figure 1. Structure of cetyl trimethylammonium bromide (CTAB) under study.

UV-melting experiments were performed on 1 μM concentration of oligonucleotides D_0 (unlabeled), D_D (tagged with 5′-fluorescein), D_A (labeled with 5′-TAMRA) and D_{DA} (tagged with 5′-fluorescein as well as 5′-TAMRA) by heating from 20 to 95 °C at a scanning rate of 1.0 °C/min. The melting profiles of the oligonucleotides were recorded by monitoring the absorbance of the complexes at 260 nm as a function of temperature using Cary 100 concentration UV−visible spectrophotometer with temperature controller. Transition temperatures (T_m) were calculated from the melting curves to gain insight into the helix−coil transition and revealed that their T_m values were in the rage of 33 to 37 °C (data not shown).

Fluorescence and FRET Studies. The fluorescence spectra of dual labeled oligonucleotide (D_{DA}) were recorded in the absence and presence of CTAB from 500 to 700 nm, at an excitation wavelength (λ_{ex}) of 490 nm and at temperature 15 °C using a spectrofluorometer (Jobin Yvon FluoroMax 3) with a Peltier thermostat. Initially, fluorescence spectra of a 1 μM concentration of fluorescein tagged strand I were recorded and mixed with the required amount of TAMRA tagged strand II to maintain equimolar concentration 1 μM in 600 μL. The corresponding duplex was prepared in the fluorescence cuvette by heat−cool treatment using a Peltier thermostat, and the spectrum was recorded. The required amount of CTAB was added to the duplex. After each addition, the resulting oligonucleotide−surfactant complexes were equilibrated for 10 min before recording of each fluorescence spectrum. The titration of the surfactant was terminated when the corresponding maximum intensity (I_{max}) of the fluorescence signal for the oligonucleotide became saturated. Similarly, fluorescence spectra of oligonucleotides containing fluorescein labeled strand I and unlabeled strand II (D_D) as well as untagged strand I and TAMRA tagged strand II (D_A) were recorded both in the absence and in the presence of CTAB at an excitation wavelength (λ_{ex}) of 490 and 520 nm respectively and at 15 °C. Fluorescence spectra were also recorded in the presence and absence of CTAB for oligonucleotides D_{DA} (fluorescence tagged strand I and TAMRA tagged strand II), D_D (fluorescence tagged strand I and untagged strand II) and D_A (untagged strand I and TAMRA tagged strand II) after mixing with 150 mM NaCl. In all the experiments, the concentration of CTAB stock solutions was chosen such that the maximum dilution of oligonucleotide−CTAB complex was maintained well within 10% due to the surfactant addition. The surfactant and oligonucleotide concentrations were calculated by including the dilution factors, which were also maintained within 10% of the initial volume (600 μL).

Ethidium Bromide Exclusion Studies. Fluorescence spectra of unlabeled duplex oligonucleotide (D_0)−ethidium bromide (EB) complex were recorded in the absence and presence of CTAB from 500 to 700 nm, at an excitation wavelength (λ_{ex}) of 480 nm. Ethidium bromide (14 μM) was mixed with 1 μM oligonucleotide solutions (1EB:1bp) in 10 mM sodium phosphate buffer at pH 7.0 and equilibrated for 10 min at 15 °C. For these experiments, a stock EB solution was prepared by dissolving 1.97 mg of EB in 1000 μL of water, and the corresponding stock concentration was determined using a Cary

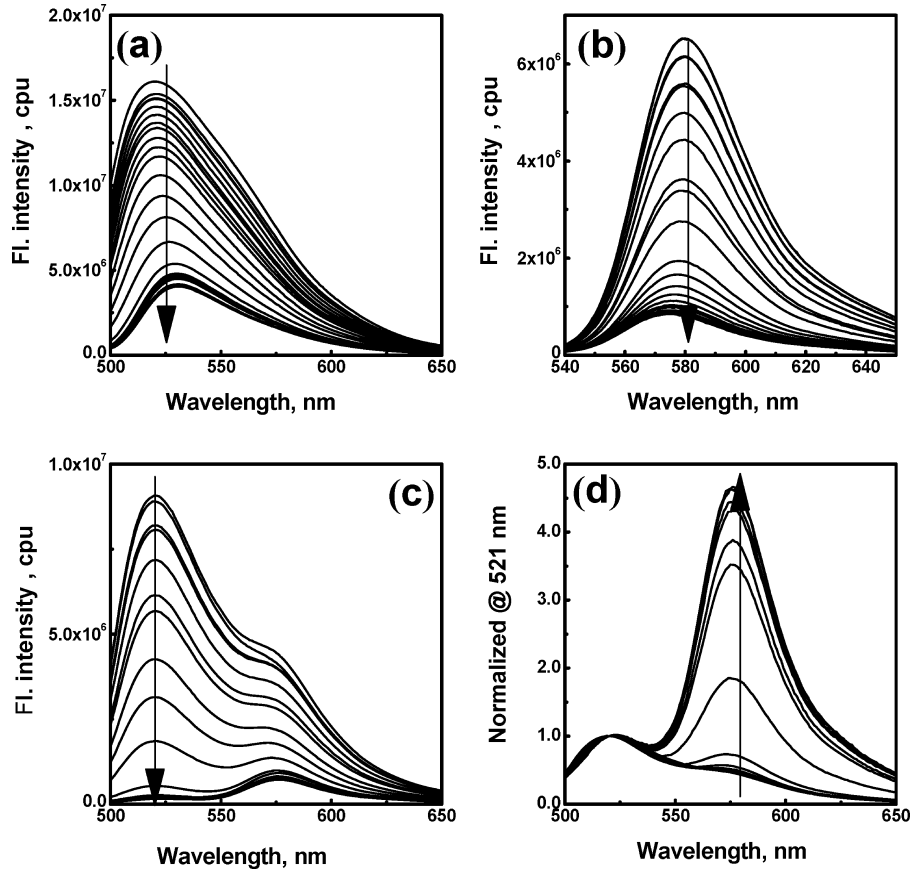

Figure 2. Fluorescence emission spectra of oligonucleotide (a) D_D (5′-fluorescein labeled), (b) D_A (5′-TAMRA labeled) and (c) D_{DA} (5′-fluorescein and 5′-TAMRA labeled) and (d) normalized spectra at 521 nm that are shown in c in the absence and presence of increasing concentrations of CTAB. The oligonucleotide concentration was 1 μM in 10 mM sodium phosphate buffer (pH 7.0). The increment of $Z_{\pm}$ is indicated by arrow heads.

100 concentration UV−visible spectrophotometer assuming molar extinction coefficient 5600 L mol^{-1} cm^{-1} at 480 nm.[27] For ethidium bromide exclusion, 600 μL of oligonucleotide−ethidium bromide mixture was taken in a cuvette and increasing amounts of CTAB were added into the mixture. After each addition of the surfactant, the mixture was incubated for 10 min before recording of each spectrum. Once again, similar to the FRET studies, dilution of oligonucleotide was maintained not more than 10%, due to the addition of the surfactant solution, and stock CTAB solutions were prepared accordingly. For each fluorometric titration, the corresponding CTAB concentration was calculated by including the dilution factor.

Gel Electrophoresis Studies. The electrophoretic mobilities of CTAB/oligonucleotide (D_0) complexes at various charge ratios ($Z_{\pm}$) in the absence and presence of 150 mM NaCl were determined by using 15% native-PAGE. Gel electrophoresis experiments were carried out in a buffer consisting of 45 mM Tris-borate and 1 mM EDTA at pH 8.0. In these studies, a 1 μM concentration of oligonucleotide (equivalent to 26 μM phosphate unit) was mixed with various concentrations of the desired surfactant solution for the preparation of the complex of required charge ratio and incubated for 30 min. Polyacrylamide gels were run at 120 V for 4 h at 4 °C. The oligonucleotide was visualized under UV illumination after staining the gels with ethidium bromide for 30 min at room temperature.

Results and Discussion

Fluorescence and FRET Studies. Fluorescence emission spectrum of duplex containing 5′-fluorescein tagged strand I and untagged strand II (D_D) were recorded in the absence and presence of increasing CTAB concentration (Figure 2a). In the absence of CTAB, the oligonucleotide (D_D) shows emission maximum at 521 nm upon excitation at 490 nm. Interestingly, a decrease in fluorescence intensity is observed for 5′-fluorescein tagged strands with increase in surfactant concentration. The observed decrease can be attributed to the microenvironmental change in the oligonucleotide−CTAB system, which results in the burial of the fluorescein molecule. After a particular concentration of CTAB, the fluorescence spectrum of the duplex does not show any change in the emission intensity, indicating saturation. Additionally, the observed red shift in the emission maxima of 5′-fluorescein tagged strands with increasing surfactant concentration indicates formation of hydrophobic assemblies.

Figure 2b shows interaction between the oligonucleotide (D_A) containing unlabeled strand I and 5′-TAMRA labeled strand II. The fluorescence emission maximum was detected at 582 nm upon excitation at 520 nm. Similar to the interaction between (D_D) and CTAB, the decrease in the fluorescence emission intensity of TAMRA was observed with increasing concentration of the cosolute. However, in contrast to D_D, the emission maxima were found to shift toward lower wavelength (blue shift). Similar to the observed red shift in fluorescein emission (Figure 2a), blue shifts in TAMRA emission are also due to the oligonucleotide−CTAB complex formation, which results in microenvironmental change from polar to nonpolar in the vicinity of the fluorophore. The opposite behavior observed for the two fluorophores was confirmed by obtaining emission

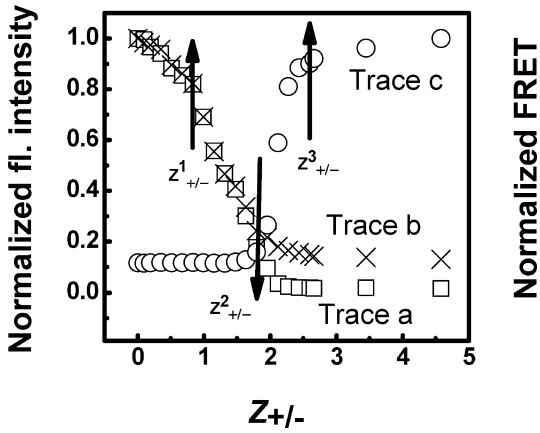

Figure 3. Fluorometric titration curves of the oligonucleotides D_D (5′-fluorescein labeled) (trace a, □), D_A (5′-TAMRA labeled) (trace b, ×) and D_{DA} (5′-fluorescein and 5′-TAMRA labeled) (trace c, ○) at various CTAB to oligonucleotide charge ratios. The oligonucleotide concentration was 1 μM in 10 mM sodium phosphate buffer (pH 7.0). Break points ($Z^1_{\pm}$, $Z^2_{\pm}$ and $Z^3_{\pm}$) are represented by arrows.

spectra of the free fluorophores in three different solvents, namely, water, methanol and hexane. In the case of fluorescein, emission maxima were 518, 521, and 524 nm in water, methanol and hexane respectively, whereas, in the case of TAMRA, emission maxima were 572, 566, and 557 nm in water, methanol and hexane respectively (data not shown). The fluorescence spectra of the oligonucleotide (D_{DA}) comprising 5′-fluorescein tagged strand I and 5′-TAMRA labeled strand II in the absence and presence of the surfactant are depicted in Figure 2c. In the absence of CTAB, as expected, the duplex under investigation shows two fluorescence emission maxima, one each at 520 and 575 nm corresponding to donor emission and acceptor emission respectively upon excitation at 490 nm. As observed earlier (Figure 2a and 2b), a decrease in the fluorescence emission intensities was reported for donor as well as acceptor up to a certain concentration increase of CTAB. Interestingly, at higher CTAB concentration, an increase in the emission intensity of TAMRA was observed. Correspondingly, emission intensity of fluorescein was found to be moderately decreasing with increasing concentration of CTAB. These observations reveal that only a small amount of resonance energy is transferred from the donor to the acceptor.

In order to show the increase in fluorescence energy emission of TAMRA at higher CTAB concentration (Figure 2c) more evidently, the corresponding individual spectrum of D_{DA} was normalized at 521 nm in the emission maxima of fluorescein (Figure 2d). Data (Figure 2d) clearly indicate that the fluorescence intensity of TAMRA does not change, upon initial addition of CTAB, relatively to the fluorescence intensity of fluorescein (Figure 2c). But on further addition of CTAB, a more prominent increase in the fluorescence intensity of TAMRA with respect to fluorescein intensity and followed by a saturation in the TAMRA energy emission is brought out in Figure 2d compared to Figure 2c. This typical behavior in the normalized fluorescence spectra of D_{DA} clearly indicates that there is no energy transfer from donor to acceptor at the initial stage, while after a certain concentration of CTAB addition, either inter- or intramolecular distance between the donor and the acceptor fluorophores decreases, because of which a resonance energy transfer between donor and acceptor occurs.

Typical curves for fluorometric titrations of duplexes D_D (trace a), D_A (trace b), and D_{DA} (trace c) with CTAB are shown in Figure 3. Here the normalized fluorescence intensity (I_{521}/I^0_{521}, where I^0_{521}, I_{521} are the fluorescence intensities of D_D in the absence and presence of CTAB from Figure 2a) was plotted as a function of $Z_{\pm}$ (represented by symbol □, trace a), where $Z_{\pm}$ is the surfactant to oligonucleotide charge ratio. Similarly, normalized fluorescence intensity (I_{580}/I^0_{580}, where I^0_{580}, I_{580} are the fluorescence intensities of D_A in the absence and presence of CTAB from Figure 2b) was plotted as a function of $Z_{\pm}$ (shown by symbol ×, trace b). For $D_{DA,}$ [I_{580}/I_{520}] values were extracted from Figure 2c and normalized with the I_{580}/I_{520} value corresponding to the highest concentration of the surfactant in order to highlight the increase in the energy emission of TAMRA (trace c) in comparison with traces a and b and then plotted against the charge ratio ($Z_{\pm}$) (represented by symbol ○, trace c). Trace a and trace b in Figure 3 provide information about the nature of interaction between the oligonucleotide and CTAB with increasing CTAB concentration. In other words, traces a and b represent two steps involved in complex formation between the duplex and CTAB, by probing microenvironment around the fluorophore attached to the oligonucleotide, whereas trace c in Figure 3 provides additional information about the distance between donor and acceptor fluorophores, during the course of interaction with the surfactant. From the figure it is evident that the titration curves of the oligonucleotide show two break points for the donor as well as the acceptor emission where the corresponding fluorescence changes sharply. Interestingly, two distinct characteristic $Z_{\pm}$ values ($Z^1_{\pm} = 0.8$, $Z^2_{\pm} = 1.7$ respectively) are found to be similar for fluorescein as well as TAMRA emission. Having two break points in trace a as well as in trace b of Figure 3 indicates that there are two steps involved when duplex interacts with CTAB.

The first step is the electrostatic interaction between surfactant monomer and negatively charged phosphate groups of the oligonucleotide. This interaction is completed at the first break point, i.e. $Z^1_{\pm} = 0.8$ in the present case. During this process a mild decrease in fluorescence intensity of duplex attached fluorophore was observed. Such decrease in fluorescence intensity of duplex is often observed when the fluorescent dye is in a hydrophobic environment.[28] After this $Z_{\pm}$, a further increase in CTAB concentration produced a sharp decrease in fluorescence intensity for both D_D and D_A duplexes, indicating formation of a stronger hydrophobic environment around the duplex upon the complex formation with CTAB. The presence of a hydrophobic environment indicates the presence of surfactant self-assembly, which could be DNA induced. This DNA-induced self-assembly continues up to a charge ratio of 1.7. Beyond this charge ratio of 1.7, there is no further change as far as microenvironment of DNA−surfactant assembly is concerned. Trace c in Figure 3 shows normal FRET as a function of $Z_{\pm}$. The absence of FRET observed up to $Z^2_{\pm} = 1.7$ indicates that TAMRA and fluorescein are far apart. A striking increase in FRET after the charge ratio 1.7 ($Z^2_{\pm}$) is indicative of decreasing distance between the donor and acceptor moieties. The highest FRET intensity at $Z^3_{\pm} = 2.5$ refers to the shortest possible either inter- or intramolecular distance between the donor and acceptor. At this stage of the interaction, condensation of the oligonucleotide by bending as well as coiling for intramolecular FRET can be ruled out due to shorter chain length of the oligonucleotide and neutralization of the oligonucleotide. It is also pertinent to mention that, based on our earlier UV-melting data on the oligonucleotide (D_0) and CTAB,[29] denaturation followed by coiling of the oligonucleotide in the presence of CTAB (up to the charge ratio $Z_{\pm} = 3$) is highly unlikely.

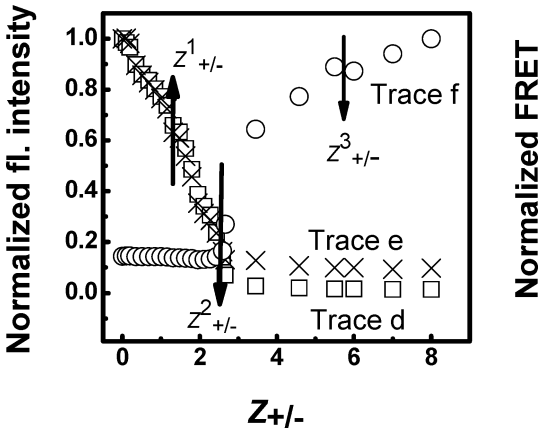

Figure 4. Fluorometric titration curves of the oligonucleotides in the presence of 150 mM NaCl. D_D (5′-fluorescein labeled) (trace d, □), D_A (5′-TAMRA labeled) (trace e, ×) and D_{DA} (5′-fluorescein and 5′-TAMRA labeled) (trace f, ○) at various CTAB to oligonucleotide charge ratios. The oligonucleotide concentration was 1 μM in 10 mM sodium phosphate buffer (pH 7.0). Break points ($Z^1_{\pm}$, $Z^2_{\pm}$ and $Z^3_{\pm}$) are represented by arrows.

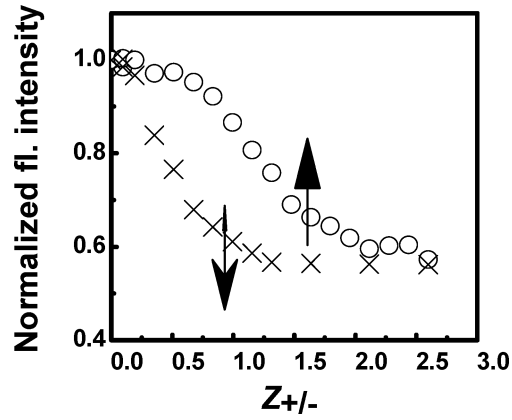

Figure 5. Ethidium bromide exclusion experiments for oligonucleotide at various CTAB to oligonucleotide charge ratios (×) in the absence of NaCl and (○) in the presence of 150 mM NaCl. Arrow heads represent arbitrary saturation points in the displacement of EB from the oligonucleotide by CTAB. The oligonucleotide concentration was 1 μM in 10 mM sodium phosphate buffer (pH 7.0).

The findings of FRET studies are further confirmed by similar fluorometric titration of D_D (represented by symbol □, trace d), D_A (shown by symbol ×, trace e), and D_{DA} (represented by symbol ○, trace f) in the presence of 150 mM NaCl (Figure 4). Here again, normalized fluorescence intensities [I_{521}/I^0_{521}], [I_{580}/I^0_{580}] and [I_{580}/I_{520}] of D_D, D_A and D_{DA} respectively in the presence of 150 mM NaCl are plotted against $Z_{\pm}$. It is worth mentioning that, similar to the pattern observed in Figure 3, three distinguishable changes in $Z_{\pm}$ values reappeared in the titration curves of oligonucleotide DNA in the presence of salt (Figure 4). Additionally, the break points were found to be shifted to higher surfactant/DNA charge ratios ($Z_{\pm}$) in comparison with that in the absence of the salt (Figure 3). For example, in the presence of NaCl, $Z^1_{\pm}$ shifts from 0.8 to 1.3 (trace d) and $Z^2_{\pm}$ shifts from 1.7 to 2.5 (trace e) (Figure 3). The FRET intensity was found to increase with increase in $Z_{\pm}$ values, and a noticeable saturation in the intensity of TAMRA emission was not observed (trace f). The observed shift in the break points toward higher charge ratios in the presence of salt can be explained as follows: In the presence of 150 mM NaCl, the effective screening of the negative charges exists along the oligonucleotide backbone by Na^+ ions and oligonucleotide segments are held closely compared to in the absence of salt. Hence, the accessibility of phosphate charges by CTAB molecules could take place only at higher CTAB concentrations.[30−32] Correspondingly, the neutralization of the oligonucleotide by the surfactant occurs at higher charge ratios ($Z^1_{\pm}$ = 1.3). Additionally, this screening effect of salt can also lead to an increase in the CAC of the surfactant,[32] which causes an increase in the second break point ($Z^2_{\pm}$ = 2.5) followed by a FRET at higher charge ratios compared to in the absence of the salt.

Ethidium Bromide Exclusion Studies. Ethidium bromide exclusion studies from DNA upon complex formation with different cationic agents such as polypeptides,[33,34] polyamines,[35] cationic dendrimers,[36] cationic polymers[37] and cationic surfactants[28,38,39] were extensively carried out in the development of nonviral gene delivery systems. In order to investigate the surfactant binding to the oligonucleotide, EB, a cationic dye, is premixed with the DNA in the absence and presence of NaCl and titrated with CTAB solution (Figure 5). The ethidium ion intercalates into the DNA and dramatically increases its fluorescence efficiency. The addition of CTAB into the DNA−EB complex solution results in the removal of the intercalated EB from the DNA molecule, and a quenching of fluorescent intensity is observed. In both the absence and presence of NaCl, the fluorescent intensity of DNA−EB premix solution decreases with increase in the surfactant concentration ($Z_{\pm}$ values) and portrays a distinct characteristic $Z_{\pm}$ value, represented by arbitrary arrow heads (Figure 5: down arrowhead in the absence of the salt (×) and up arrowhead in the presence of the salt (○)). The characteristic $Z_{\pm}$ values in the absence of NaCl (0.8) and in the presence of NaCl (1.5) are decided based on gel electrophoresis studies (Figure 6). It is also noteworthy that binding of CTAB to DNA-phosphate sites was reported up to the charge ratio (CTAB/DNA-phosphate) of about 0.7 to 0.8 by Chaires et al.[40] Since $Z_{\pm}$ is the charge ratio when the oligonucleotide is saturated with the surfactant molecule, no further binding to oligonucleotide can occur on further addition of surfactant to the solution and, therefore, no more exclusion of EB from oligonucletides could be observed. In the presence of NaCl, the observed increase in the saturation value ($Z_{\pm}$ = 1.5) is higher in comparison with the saturation value ($Z_{\pm}$ = 0.8) in the absence of NaCl, which is again attributed to the screening effect of Na^+ ions on the oligonucleotide and the increased oligonucleotide stability.[30−32] It is noteworthy to recall that, in the fluorometric titration of various oligonucleotides with CTAB (Figures 3 and 4) in the absence and presence of NaCl, the charge neutralization values ($Z^1_{\pm}$) were found to be 0.8 and 1.3 (Figures 3 and 4), respectively, which are in good agreement with the saturation values in EB exclusion studies ($Z_{\pm}$ = 0.8 and $Z_{\pm}$ = 1.5) both in the absence and in the presence of NaCl respectively.

Gel Electrophoresis Studies. Gel electrophoresis is one of the important tools to study the size and charge of DNA and can also be utilized to study the interaction between DNA and the oppositely charged ligands. In the absence of NaCl (Figure 6a), the oligonucleotide band migration could be seen until the surfactant to oligonucleotide charge ratio of 0.75 ($Z_{\pm}$). It is also relevant to mention that the intensity of oligonucleotide band gradually decreases with increase in charge ratio. Similarly, in the presence of NaCl, the band until the charge ratio of 1.5 ($Z_{\pm}$) and the band migration is not seen at and above the charge ratio ($Z_{\pm}$) of 2. From the observations, it can be concluded that, in the absence and presence of NaCl, the oligonucleotide DNA carries a negative charge at charge ratio of ≤0.75 and ≤1.5 respectively and charge neutralization occurs beyond this point.

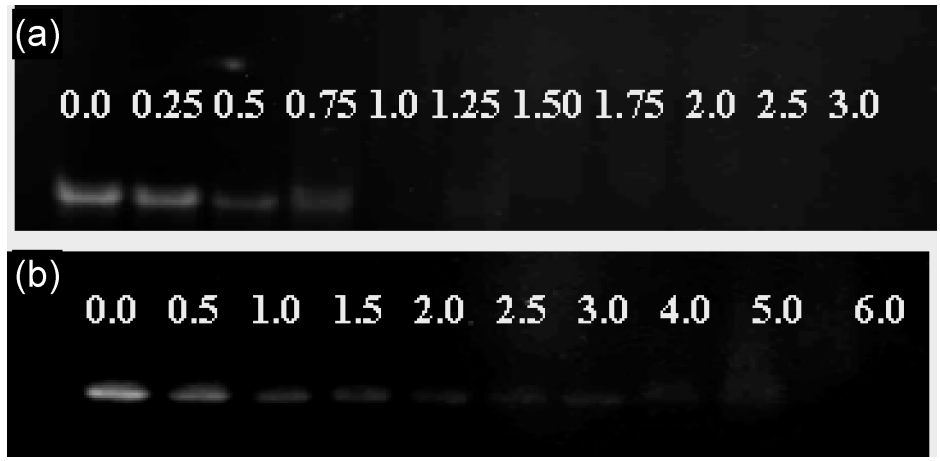

Figure 6. Gel electrophoresis assay. 15% nondenaturing PAGE was run with complexes of CTAB (a) in the absence of NaCl and (b) in the presence of 150 mM NaCl at various CTAB to oligonucleotide charge ratios (as mentioned on the corresponding lanes). The gel was run in buffer consisting of 45 mM Tris-borate and 1 mM EDTA at pH 8.0, at 120 V for 60 min at 4 °C. The gels were visualized under UV illumination after staining with ethidium bromide at room temperature.

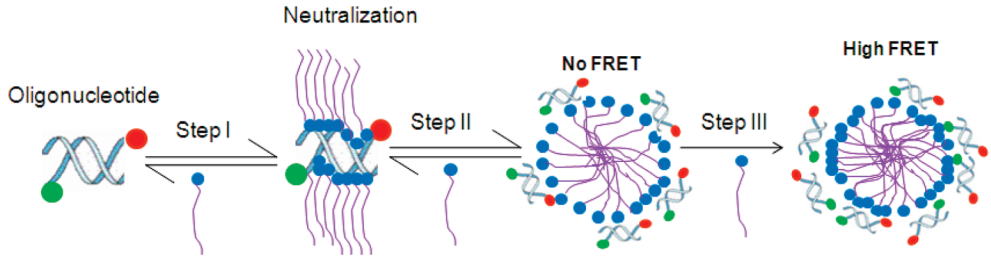

Figure 7. A schematic diagram of the oligonucleotide−CTAB interaction.

Moreover, a gradual decrease in the intensity of the duplex bands with increase in the concentration of CTAB indicates neutralization of DNA by surfactant to various extents.

Overall, various biophysical techniques are used to study the interaction between DNA and oppositely charged ligands, and different techniques give different types of information.[1] For example, the binding of cationic agent with DNA−EB complex resulted in a competitive displacement of the intercalated EB from the double helix to the solution. The observed EB displacement is indicated by a fluorescence quenching and provides information on the electrostatic interactions between cationic agent and DNA. Gel electrophoresis studies allow visualization of the interaction of DNA and cationic agents providing the charge neutralization point between DNA and cationic agents. However, these extensively used techniques fail to probe detailed structural changes in the DNA. It is also worth mentioning that fluorescence microscopy (FM) as well as dynamic light scattering (DLS) revealed about three distinguishable regimes in DNA conformational changes depending on the surfactant concentration. In essence, there exist distinct free DNA coils, coexistence of coiled as well as globular DNA molecules and finally DNA in mere compact form with increasing concentration of the surfactant.[18,41,42] It is also noticeable that FM as well as DLS could not probe packaging of surfactant molecules in and around DNA.

On the other hand, it is interesting to note that only FRET studies reveal additional information during the oligonucleotide and surfactant interaction such as DNA induced self-assembly of the surfactant and the intermolecular energy transfer between donor and acceptor fluorophores due to the difficulty in conformational changes of the 14mer oligonucleotide in addition to neutralization of the oligonucleotide by the surfactant.

Surfactant and DNA Interaction Mechanisms. Based on the results, a definite conclusion regarding structural aspects of oligonucleotide−CTAB complexes at various stages of the surfactant binding to the 14mer can be drawn (Figure 7). Step I involves the binding of the CTAB molecules with the DNA by electrostatic attraction and neutralization of charge at $Z_{\pm} = 0.8$. These observations are in good agreement with previous reports, which reveal that interaction between the cationic surfactant and the DNA is very similar to the binding of oppositely charged ligands to other polyelectrolytes.[1] It is worth recalling that at $Z_{\pm} = 0.8$, the first break point was observed in fluorometric titrations ($Z^1_{\pm}$ trace a and trace b, Figure 3) which is shown by slight decrease in fluorescence intensity of duplex indicating hydrophobic environment around the fluorescent dye. The following sharp decrease in fluorescence intensity above the charge ratio 0.8 shows the formation of stronger hydrophobic environment around the fluorophore (Figure 3). Hence, it is inferred that further addition of CTAB just above this neutralization point ($Z_{\pm} > 0.8$) would result in binding of new surfactant molecules to the neutralized oligonucleotide−CTAB complexes which then undergoes oligonucleotide induced self-assembly to form micellar aggregates. This step corresponds to the second step (Figure 7). Such micellar aggregation of CTAB in the vicinity of the oligonucleotide completes at $Z_{\pm} = 1.7$, which is indicated by the second break point $Z^2_{\pm}$ in fluorometric titration of D_D (trace a) and D_A (trace b) with CTAB (Figure 3). This huge energy transfer observed by FRET experiments at the charge ratio range of 1.7 to 2.5 ($Z_{\pm}$) (trace c, Figure 3) corresponds to the third step in the surfactant−oligonucleotide interaction (Figure 7). The observed resonance energy transition in the profile most probably can be attributed to an increase in the number of oligonucleotide molecules per micellar aggregates. This may happen due to an increase in the number of loosely held surfactant aggregates with increase in the surfactant concentration and eventually causes the fusion of micelles. In addition to this, micellar shape may also undergo a change.[43]

Such a change in geometry of surfactant aggregates is speculated as it will allow for more effective distribution of oligonucleotides around the available micelles. The local concentration of the oligonucleotide along each micelle would hence increase and the end-to-end distance between two oligonucleotide molecules will decrease, which manifests as a marked increase in the energy transfer, as observed (Figure 7). However, determination of number of surfactant aggregates as well as understanding the shape of oligonucleotide-surfactant aggregates will give better interpretation of the results.

Conclusion

In this study, the interaction mechanisms between the 14mer oligonucleotide and CTAB molecules have been studied based on fluorescence and FRET studies. The observations indicate three steps in oligonucleotide−CTAB interactions. Initially, the oligonucleotide is neutralized by the CTAB molecules. Interestingly, further addition of surfactant led to micellar aggregation of CTAB in the vicinity of the oligonucleotide. Finally at higher the surfactant concentration, there seems to be an increase in the number of micellar aggregation followed by a fusion of these loosely held aggregates. Additionally, there may be a micellar shape change that allows a higher and effective accommodation of oligonucleotide around the micelles and a consequent decrease in the intermolecular distance between the oligonucleotides, leading to a higher fluorescence energy transfer. In the presence of salt, it was evident that a higher concentration of CTAB was required for the neutralization of the oligonucleotide than was required in absence of salt, owing to the screening effect. It is significant to mention that most of the reported techniques such as ethidium bromide exclusion as well as gel electrophoresis could probe only up to the neutralization of the oligonucleotide by the surfactant molecules, while study shown here extends to DNA induced self-assembly of the surfactant and explains about the oligonucleotide−surfactant aggregates.

Acknowledgment. Financial support for this work (CSIR young scientist award project) from the Council of Scientific and Industrial Research, Government of India, New Delhi, is gratefully acknowledged.

References and Notes

(1) *DNA Interaction with Polymers and Surfactants*; Dias, R. S., Lindman, B., Eds.; John Wiley and Sons: Hoboken, NJ, 2008.
(2) Anderson, W. F. *Science* **1992**, *256*, 808.
(3) Mulligan, R. C. *Science* **1993**, *260*, 926.
(4) Hanania, E. G.; Kavanagh, J.; Hortobagyi, G.; Giles, R. E.; Champlin, R.; Deisseroth, A. B. *Am. J. Med.* **1995**, *99*, 537.
(5) Nishikawa, M.; Huang, L. *Hum. Gene Ther.* **2001**, *12*, 861.
(6) Luo, D.; Saltzman, W. M. *Nat. Biotechnol.* **2000**, *18*, 33.
(7) Zuber, G.; Dauty, E.; Nothisen, M.; Belguise, P.; Behr, J. P. *Adv. Drug Delivery Rev.* **2001**, *52*, 245.
(8) Maurer, N.; Fenske, D. B.; Cullis, P. R. *Expert Opin. Biol. Ther.* **2001**, *1*, 923.
(9) Ganguli, M.; Jayachandran, K. N.; Maiti, S. *J. Am. Chem. Soc.* **2004**, *126*, 26.
(10) Raper, S. E.; Chirmula, N.; Lee, F. S.; Wivel, N. A.; Bagg, A.; Gao, G.-P.; Wilson, J. M.; Batshaw, M. L. *Mol. Genet. Metab.* **2003**, *80*, 148.
(11) Hacein-Bey-Abina, S.; von Kalle, C.; Schmidt, M.; Le Deist, F.; Wulffraat, N.; McIntyre, E.; Radford, I.; Villeval, J.-L.; Fraser, C. C.; Cavazzana-Calvo, M.; Fischer, A. *New Engl. J. Med.* **2003**, *348*, 255.
(12) Bloomfield, V. A. *Biopolymers* **1997**, *44* (3), 269.
(13) Yoshikawa, Y.; Yoshikawa, K.; Kanbe, T. *Langmuir* **1999**, *15*, 4085.
(14) Arscott, P. G.; Ma, C.; Wenner, J. R.; Bloomfield, V. A. *Biopolymers* **1995**, *36*, 345.
(15) Osica, V. P.; Pyatigorskaya, T. L.; Polyvtsev, O. F.; Dembo, A. T.; Klija, M. O.; Vasilchenko, V. N.; Venkin, B. I.; Ya, B. *Nucleic Acids Res.* **1977**, *4*, 1083.
(16) Hayakawa, K.; Santerre, J. P.; Kwak, J. C. T. *Biophys. Chem.* **1983**, *17*, 175.
(17) Morimoto, M.; Ferchmin, P. A.; Bennett, E. L. *Anal. Biochem.* **1978**, *62*, 436.
(18) Mel'nikov, S. M.; Sergeyev, V. G.; Yoshikawa, K. *J. Am. Chem. Soc.* **1995**, *117*, 9951.
(19) Mel'nikov, S. M.; Sergeyev, V. G.; Yoshikawa, K. *Recent Res. Dev. Chem. Sci.* **1997**, *1*, 69.
(20) Mel'nikov, S. M.; Sergeyev, V. G.; Yoshikawa, K.; Takahashi, H.; Hatta, I. *J. Chem. Phys.* **1997**, *107*, 6917.
(21) Mel'nikov, S. M.; Yoshikawa, K. *Biochem. Biophys. Res. Commun.* **1997**, *230*, 514.
(22) Mel'nikova, Y. S.; Lindman, B. *Langmuir* **2000**, *16*, 5871.
(23) Dias, R.; Mel'nikov, S.; Lindman, B.; Miguel, M. G. *Langmuir* **2000**, *16*, 9577.
(24) Le Ny, A. L. M.; Lee, C. T., Jr. *J. Am. Chem. Soc.* **2006**, *128*, 6400.
(25) Marky, L. A.; Blumenfeld, K. S.; Kozlowski, S.; Breslauer, K. *J. Biopolym.* **1983**, *22*, 1247.
(26) Kaur, H.; Arora, A.; Wengel, J.; Maiti, S. *Biochemistry* **2006**, *45*, 7347.
(27) Waring, M. J. *J. Mol. Biol.* **1965**, *13*, 269.
(28) Chanb, V.; McKenzied, S. E.; Surrey, S.; Fortina, P.; Graves, D. J. *J. Colloid Interface Sci.* **1998**, *203*, 197.
(29) Jadhav, V. M.; Valaske, R.; Maiti, S. *J. Phys. Chem. B* **2008**, *112*, 8824.
(30) Marky, L. A.; Patel, D.; Breslauer, K. J. *Biochemistry* **1981**, *20*, 1427.
(31) Schlick, T.; Li, B.; Olson, W. K. *Biophys. J.* **1994**, *67*, 2146.
(32) Rosa, M.; Dias, R.; R. S.; Miguel, M. G.; Lindman, B. *J. Phys. Chem. B* **2005**, *6*, 2164.
(33) Wyman, T. B.; Nicol, F.; Zelphati, O.; Scaria, P. V.; Plank, C.; Szoka, F. C. *Biochemistry* **1997**, *36*, 3008.
(34) Plank, C.; Tang, M. X.; Wolfe, A. R.; Szoka, F. C. *Hum. Gene Ther.* **1999**, *10*, 319.
(35) Tang, M. X.; Szoka, F. C. *Gene Ther.* **1997**, *4*, 823.
(36) Chen, W.; Turro, N. J.; Tomalia, D. A. *Langmuir* **2000**, *16*, 15.
(37) Nisha, C. K.; Sukara, V. M.; Ganguli, M.; Maiti, S.; Kizhakkedathu, J. N. *Langmuir* **2004**, *20*, 2386.
(38) Dasgupta, A.; Das, P. K.; Dias, R. S.; Miguel, M. G.; Lindman, B.; Jadhav, V. M.; Gnanamani, M.; Maiti, S. *J. Phys. Chem. B* **2007**, *111*, 8502.
(39) Jadhav, V. M.; Maiti, S.; Dasgupta, A.; Das, P. K.; Dias, R. S.; Miguel, M. G.; Lindman, B. *Biomacromolecules* **2008**, *9*, 1852.
(40) Spink, C. H.; Chaires, J. B. *J. Am. Chem. Soc.* **1997**, *119*, 10920.
(41) Yoshikawa, K.; Takahashi, M.; Vasilevskaya, V. V.; Khokhlov, A. R. *Phys. Rev. Lett.* **1996**, *76*, 3029.
(42) Mel'nikov, S. M.; Sergeyev, V. G.; Yoshikawa, K. *J. Am. Chem. Soc.* **1995**, *117*, 2401.
(43) Svensson, A.; Norrman, J.; Piculell, L. *J. Phys. Chem. B* **2006**, *110*, 10332.

JP909522R